

Final Report for PAS NASA 3

NAG8 1223

## Passive accelerometer system measurements on MIR

J. Iwan D. Alexander

Principal Investigator

Center for Microgravity and Materials Research

University of Alabama in Huntsville, Huntsville, Alabama 35899

### Abstract

The passive accelerometer system (PAS) is a simple moving ball accelerometer capable of measuring the small magnitude steady relative acceleration that occurs in a low earth orbit spacecraft due to atmospheric drag and the earth's gravity gradient. The acceleration is measured by recording the average velocity of the spherical ball over a suitable time increment. A modified form of Stokes law is used to convert the average velocity into an acceleration. PAS was used to measure acceleration on the MIR space station and on the first United States Microgravity Laboratory (USML-1). The PAS measurement on MIR revealed remarkably low acceleration levels in the SPEKTR module.

### Introduction

The passive accelerometer system (PAS) was designed to measure the quasi-steady residual acceleration caused by a combination of atmospheric drag effects and the gravity gradient. These accelerations are typically on the order of  $10^{-6} - 10^{-5} \text{ m s}^{-2}$ , that is  $10^7 - 10^6$  times the acceleration one experiences at the earth's surface and are difficult to measure using conventional accelerometers. The acceleration is obtained indirectly by recording the motion of a small sphere along an oriented tube filled with liquid. The trajectory and speed of the sphere can then be used to find the residual acceleration indirectly using Stokes' Law [1-3]. Since the walls of the PAS tube affect the motion of the sphere, the Ladenburg-Faxen-Francis [4] correction to Stokes' Law is used.

### The PAS measurement

Consider a rigid sphere moving in a viscous liquid subject to the drag force due to the liquid and apparent forces arising from gravity gradient acceleration, spacecraft attitude motion, atmospheric drag on the spacecraft. The equations governing this motion are non dimensionalized using  $(a_0^3 / GM_e)^{1/2}$  and  $d$  as scale factors for time and distances within the spacecraft, where  $G$  is the gravitational constant,  $M_e$  is the earth's mass and  $a_0$  is a characteristic orbital radius. The

gravitational force per unit mass acting on the spacecraft (and the sphere) is assumed to be a simple  $1/r^2$  type and is scaled by  $GM_e/a_0^2$ . The resulting equations have the form [2]

$$\ddot{\mathbf{x}} = \delta[\mathbf{G}\mathbf{z} + \dot{\mathbf{Q}}\mathbf{x} - \mathbf{Q}^2\mathbf{x} + 2\mathbf{Q}\dot{\mathbf{x}} + \mathbf{f}_d] - \alpha\dot{\mathbf{x}}, \quad (1)$$

where the ‘dot’ overscript denotes a time derivative, the gravity gradient tensor  $\mathbf{G}$  is defined by

$$\mathbf{F}(\mathbf{r}) - \mathbf{F}(\mathbf{r}_0) = \nabla\mathbf{F}(\mathbf{r}_0)(\mathbf{r} - \mathbf{r}_0) + O(|\mathbf{r} - \mathbf{r}_0|^2) = \mathbf{G}\mathbf{x} + O(|\mathbf{r} - \mathbf{r}_0|^2), \quad (2)$$

and  $\mathbf{r}$  is the position vector for the earth’s mass center to a point in the spacecraft,  $\mathbf{r}_0$  is the position vector to the spacecraft mass center,  $\mathbf{x}$  is the location of the sphere relative to the center of mass of the spacecraft,  $\mathbf{G}$  is the gravity gradient acceleration associated with the nondimensionalized gravitational force,  $\mathbf{F} = \mathbf{r}/r^3$ ,  $\mathbf{Q}$  is the rate of rotation tensor for a given orbital attitude and  $\mathbf{f}_d$  is the relative acceleration due to atmospheric drag on the spacecraft. The parameters  $\alpha$  and  $\delta$  are, respectively, the non-dimensional Stokes and buoyancy coefficients and are given by

$$\alpha = \frac{9}{2} \frac{\mu}{\rho R^2} k_w \left( \frac{a_0^3}{\gamma} \right)^{1/2}, \quad \delta = \frac{\rho_s - \rho_L}{\rho}, \quad \rho = \rho_s - 1/2\rho_L, \quad k_w = \left( 1 - \frac{R}{R_w} \right)^{-2.5}, \quad (3)$$

where  $\mu$  is the shear viscosity of the liquid,  $R$  and  $R_w$  are the radii of the sphere and the accelerometer tube,  $k_w$  is the Ladenburg-Faxen-Francis correction [6] which accounts for the retardation of the sphere’s motion due to the tube walls and  $\rho_s$  and  $\rho_L$  are the densities of the sphere and the liquid, respectively. The effects of added mass [4] are included in  $\rho$ .

The apparent forces in (1) arise due to the fact that the observer’s frame of reference is attached to the spacecraft which is in low earth orbit (see Fig. 1). The form of these apparent forces depends on the spacecraft’s attitude motion and local deviations from that motion [2]. The attitude motion of the MIR space station is characterized by an inertial attitude designed to optimize use of the solar panels. The form of the equations of motion (1) for an ideal inertial orbit are

$$\ddot{x}_k(t) = \delta[G_{km}(t) x_m(t) - f_{(d)k}] - \alpha\dot{x}_k(t), \quad (4)$$

where

$$G_{km}(t) = \frac{1}{r_0^3(t)} \begin{pmatrix} 3\cos^2\theta - 1 & 0 & 3\sin\theta \cos\theta \\ 0 & -1 & 0 \\ 3\sin\theta \cos\theta & 0 & 3\sin^2\theta - 1 \end{pmatrix},$$

$$f_{(d)k} = \frac{a_0}{\varepsilon} \beta \rho_{at} (\dot{r}_0^2 - r_0^2 \dot{\theta}^2)^{1/2} \begin{pmatrix} \dot{r}_0 \cos\theta - r_0 \dot{\theta} \sin\theta \\ 0 \\ \dot{r}_0 \sin\theta - r_0 \dot{\theta} \cos\theta \end{pmatrix}. \quad (5)$$

Here  $\beta$  is an effective drag coefficient for the spacecraft,  $r_0(t)$  is the dimensionless radius of the spacecraft orbit ( $r_0(t) = 1$  for a spherical orbit of radius  $a_0$ ),  $\varepsilon = d/a_0$ , and  $\rho_{at}$  is the atmospheric density. In (4), the  $x_1$  and  $x_3$  coordinates lie in the orbit plane. The variable  $\theta(t)$  is the angular position of the spacecraft. In general, both  $\theta(t)$  and  $r_0(t)$  must be determined by solving the equations of motion subject to atmospheric drag [3,7,8]. Figure 2 shows a comparison between a computed trajectory for a 4mm diameter sphere corresponding to the PAS sphere in water with  $k_w = 1.0$ , and a trajectory computed by assuming the acceleration of the sphere to be negligible, setting the right-hand side of (4) to zero and integrating the velocity. The differences between the two trajectories are small. For the range of motions to be measured by PAS it appears that the assumption of a Stokes flow is justified and that the relative acceleration can be determined from a measurement of the sphere's velocity using the relationship

$$\langle a_i \rangle_{k_i} = \frac{\alpha}{\delta} \langle \dot{x}_i \rangle_{k_i}, \quad (6)$$

which is simply the average acceleration in the direction of the unit vector  $k$  over a specified time interval determined from the recorded average velocity.

The PAS accelerometer is used to record the motion of a small sphere along an oriented tube filled with liquid. Provided that the tube is oriented along the net acceleration direction, and provided that orientation of the acceleration does not change significantly over the measurement period, the average velocity of the sphere measured using PAS should yield a reasonable estimate of the quasi-steady residual acceleration. Any spacecraft with an orbital attitude that involves a continuous rotation of the spacecraft at a frequency equal to the orbital frequency about an axis perpendicular to the orbit plane will, to zeroth order, lead to a gravity gradient acceleration vector that, any given location in the spacecraft, has a steady magnitude and orientation. The so-called 'gravity gradient' attitude is a good example of this. The equations of motion in a gravity gradient frame of reference have the form of (1) with

$$G_{km}(t) = \frac{1}{r_0^3(t)} \begin{pmatrix} 3 & 0 & 0 \\ 0 & -1 & 0 \\ 0 & 0 & 0 \end{pmatrix}, \quad Q_{km} = \dot{\theta} \begin{pmatrix} 0 & 0 & 1 \\ 0 & 0 & 0 \\ -1 & 0 & 0 \end{pmatrix},$$

$$Q_{km} Q_{ml} = \dot{\theta}^2 \begin{pmatrix} 1 & 0 & 0 \\ 0 & 0 & 0 \\ 0 & 0 & 1 \end{pmatrix}, \quad \dot{Q}_{km} = \ddot{\theta} \begin{pmatrix} 0 & 0 & 1 \\ 0 & 0 & 0 \\ -1 & 0 & 0 \end{pmatrix} \quad (7)$$

$$f_{(d)k} = \frac{a_0}{\varepsilon} \beta \rho_{at} (\dot{r}_0^2 - r_0^2 \dot{\theta}^2)^{1/2} \begin{pmatrix} \dot{r}_0 \\ 0 \\ r_0 \dot{\theta} \cos \theta \end{pmatrix}.$$

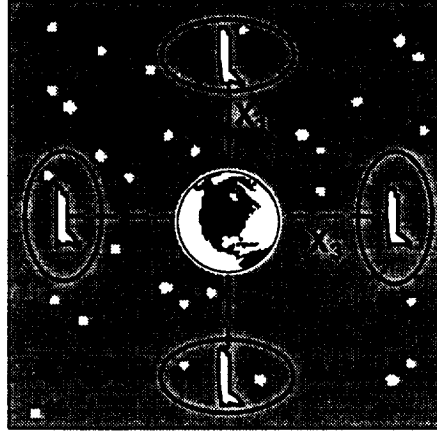
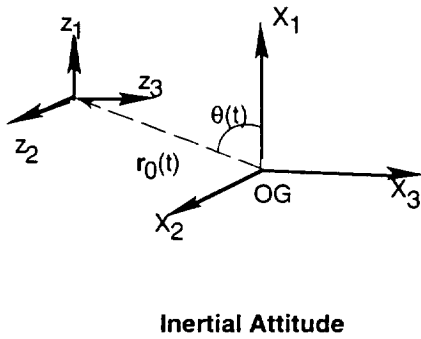
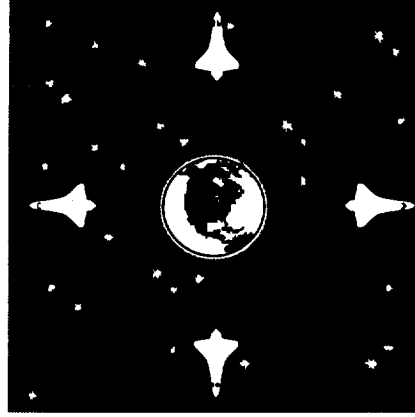
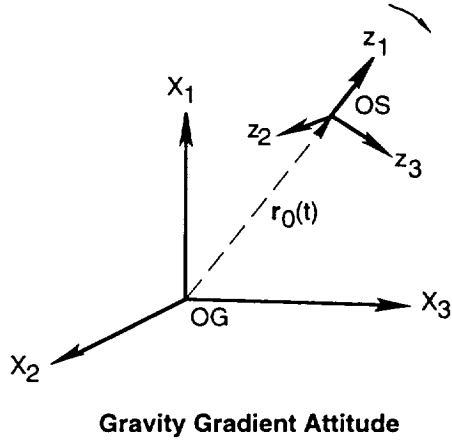


Figure 1. Spacecraft reference frames for gravity gradient and inertial attitudes.  $OG$  denotes the origin of an earth centered inertial frame. The vector  $r_0(t)$  points to the spacecraft mass center. The ellipse drawn around the spacecraft in the inertial attitude represents a section through a prolate isoacceleration surface characteristic of the gravity gradient tensor.

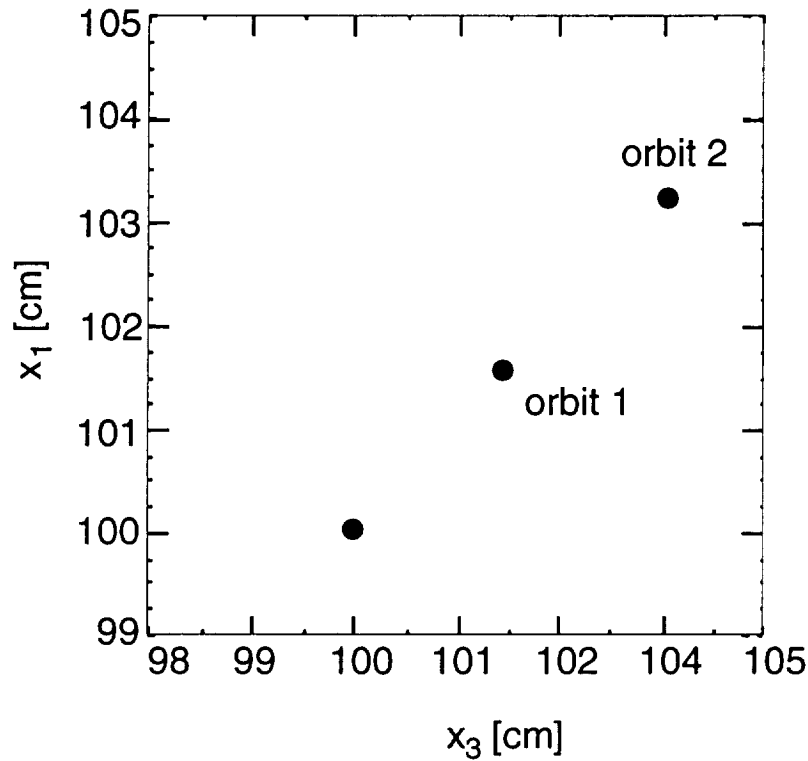


Fig. 2 Typical trajectory of a 2mm radius sphere in water. The motion is not affected by walls.

Even in a gravity gradient-type attitude, the acceleration will fluctuate due to local variations in atmospheric density but, in general, these types of attitudes can provide conditions which allow PAS to make an unambiguous acceleration measurement. It is also possible, to make acceleration measurements using PAS even when the attitude motions are of the inertial type, provided that the accelerometer is sufficiently close to the spacecraft mass center that displacements of the spherical sphere are small, or that the motion of the sphere is very rapid. This point will be addressed further in the discussion of the results from MIR.

### Apparatus and operation

The PAS consists of a 2 cm diameter glass tube with a wall thickness of 2mm. The tube is filled with water and contains a 0.4 cm diameter steel ball. At one end of the tube is a “fill and pump port” with a high vacuum stopcock valve. The inner glass tube is enclosed in a clear LEXAN tube (see Fig. 3). The LEXAN tube is sealed with two endcaps and is attached to modified camera tripod head to allow for a full range of orientations. The tripod head is mounted

onto a steel plate which is backed with Velcro strips to allow for easy mounting to surfaces in the spacecraft. A pencil magnet is used to reposition the ball inside the tube.

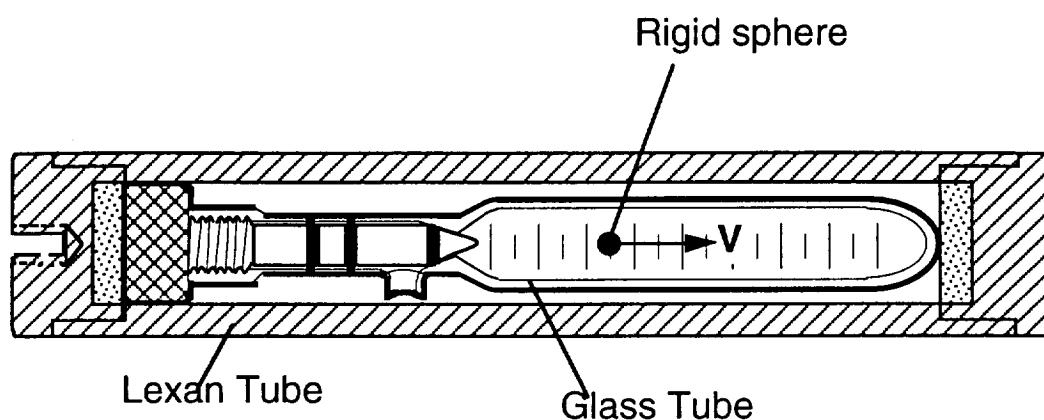


Figure 3. The passive accelerometer.

A typical operation of PAS proceeds as follows:

The accelerometer tube is oriented such that the tube axis is approximately parallel to the estimated acceleration direction (for locations in the vicinity of the spacecraft mass center, the approximate velocity vector is a good default. The magnet is then used to position the sphere at the end of the tube. The starting position of the sphere is then recorded and a timer is started. At 1-2 minute intervals the payload specialist checks that the trajectory of the sphere lies along the tube axis and records the time and position of the sphere. If the angular deviation of the ball's trajectory from the tube axis is greater than 10 degrees, the tube is repositioned such that its axis lies along the trajectory of the sphere. Each run is complete when the sphere has traversed at least 3 cm..

## Results

This section summarizes accelerometer readings made on the MIR space station from October-December 1996. For comparative purposes, results from STS-50 (USML-1) are also presented.

### *MIR residual accelerations*

PAS was deployed on 10 separate occasions between October 20 and December 17, 1996. Of the 10 measurement attempts 6 produced definite measurements. On 4 occasions, no visible motion was observed over a periods of 10-15 minutes. The results for the 6 sets of measured accelerations are shown in Table 1 and Fig. 4.

Table 1. MIR data

<b>U [m s<sup>-1</sup>]</b>	<b>acceleration [m s<sup>-2</sup>]</b>	<b>acceleration [<math>\mu</math>g]</b>	<b>Location/date</b>
1.021	$1.822 \times 10^{-5}$	$1.8593 \times 10^{-6}$	10/21/96 12:21:22
1.13	$2.029 \times 10^{-5}$	$2.0706 \times 10^{-6}$	
0.53476	$9.549 \times 10^{-6}$	$9.7442 \times 10^{-7}$	
0.27778	$4.960 \times 10^{-6}$	$5.0615 \times 10^{-7}$	
0.0292	$5.214 \times 10^{-7}$	$5.3202 \times 10^{-8}$	
0.65359	$1.167 \times 10^{-5}$	$1.1910 \times 10^{-6}$	10/25/96 15:57:00
0.48900	$8.732 \times 10^{-6}$	$8.9103 \times 10^{-7}$	
0.18349	$3.277 \times 10^{-6}$	$3.3434 \times 10^{-7}$	
0.12987	$2.319 \times 10^{-6}$	$2.3664 \times 10^{-7}$	10/28/96 15:58:40
0.12987	$2.319 \times 10^{-6}$	$2.3664 \times 10^{-7}$	
0.11765	$2.101 \times 10^{-6}$	$2.1437 \times 10^{-7}$	
0.13889	$2.480 \times 10^{-6}$	$2.5308 \times 10^{-7}$	10/29/96 14:50:30
0.26667	$4.762 \times 10^{-6}$	$4.8591 \times 10^{-7}$	
0.13605	$2.430 \times 10^{-6}$	$2.4791 \times 10^{-7}$	
0.17921	$3.200 \times 10^{-6}$	$3.2655 \times 10^{-7}$	12/16/96 15:28.02
0.049020	$8.754 \times 10^{-7}$	$8.9321 \times 10^{-8}$	
0.23256	$4.153 \times 10^{-6}$	$4.2376 \times 10^{-7}$	12/17/96 14:38:10
0.089888	$1.605 \times 10^{-6}$	$1.6379 \times 10^{-7}$	

The accelerations never exceeded  $1.9 \mu\text{g}$  and were as low as  $5 \times 10^{-2} \mu\text{g}$ . Given that the gravity gradient acceleration varies at a rate of  $0.1 \mu\text{g}$  per meter from the mass center of the spacecraft and given that the measurements that produced the highest accelerations were made in the same location that yielded PAS measurements almost an order of magnitude lower. There are two possible explanations for this,. The first is that PAS was either located near the center of mass and that the variation in acceleration magnitude was due to different drag conditions. Alternatively, other acceleration sources, such as magnetic fields may have retarded the motion of the sphere during some of the measurements. Indeed this argument seems appealing as an explanation of the observations of no-motion. However, simulations of the anticipated motion of sphere in the vicinity of the mass center of the spacecraft (within 10-100 cm) and for a range of drag magnitudes, show that it is quite possible that in the quasi-inertial attitudes flown by MIR, periods

of practically no-observable motion can occur when the drag accelerations are low enough (see Fig. 5).

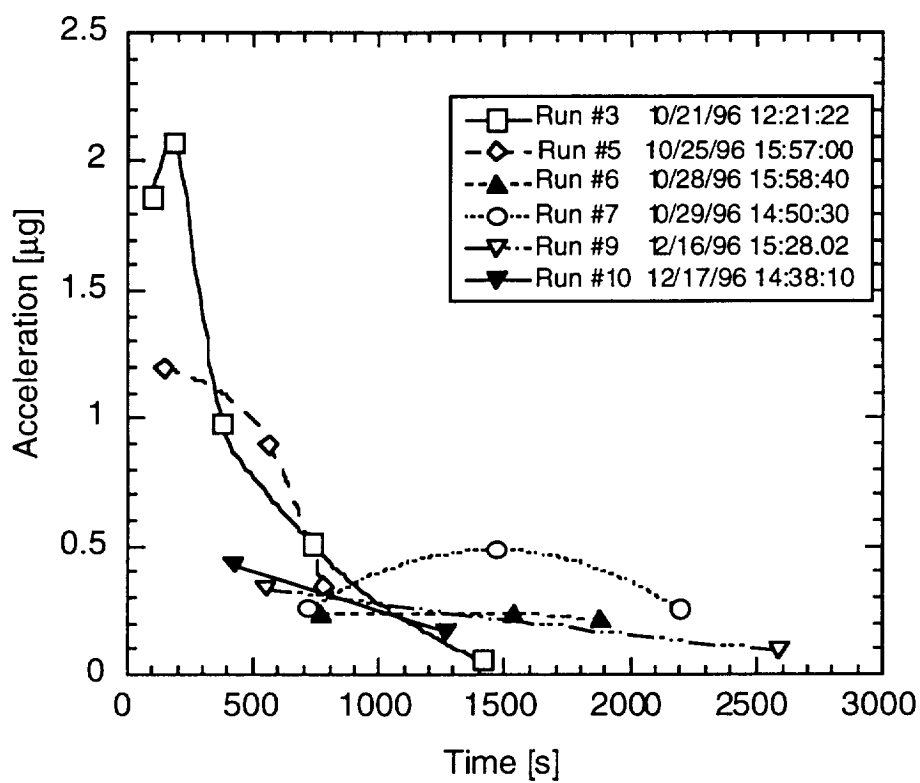


Fig. 4 PAS acceleration measurements on MIR October-December, 1996. Points are connected to show sequential measurements.



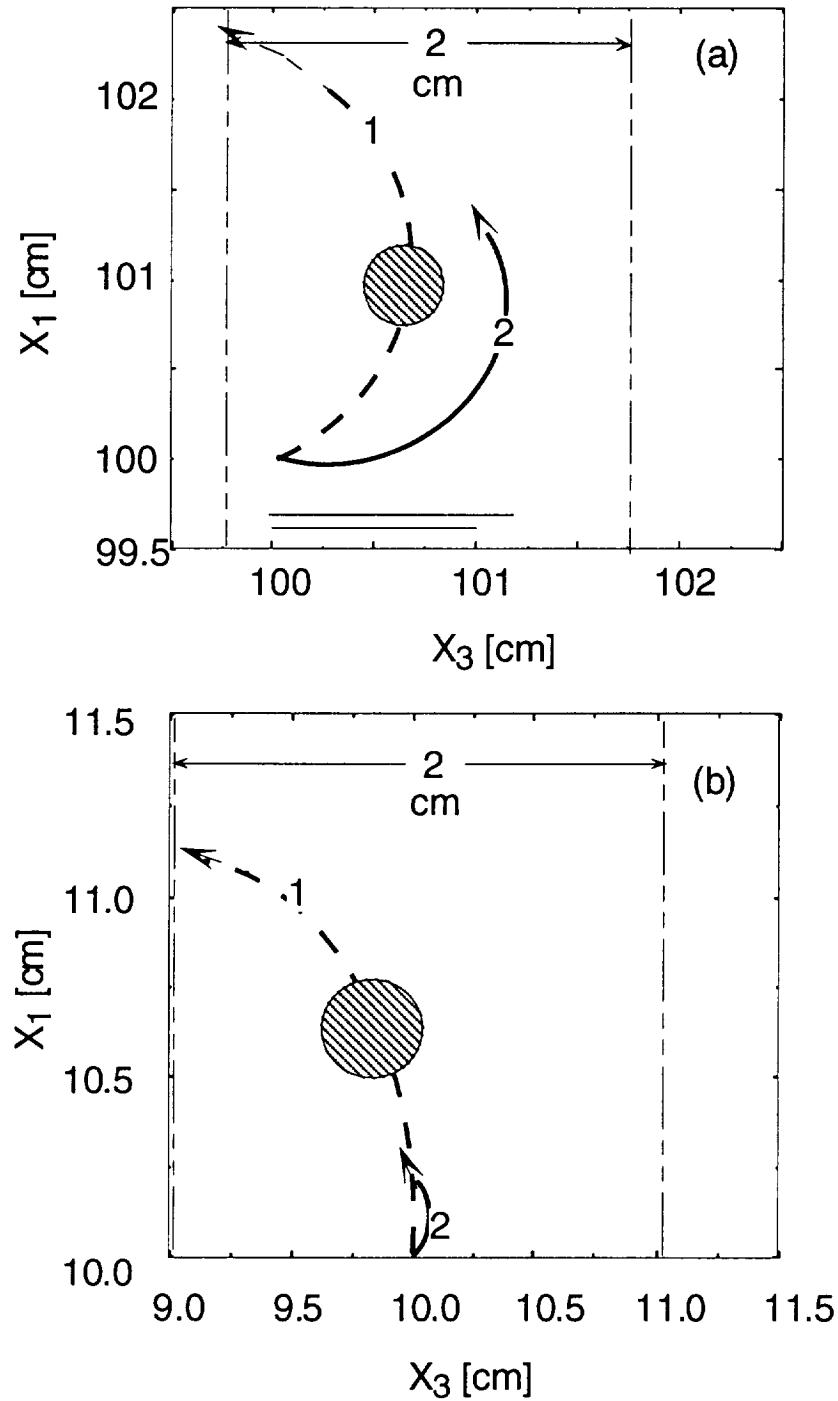


Figure 5. Trajectories of a 4 mm diameter PAS sphere released at (a)  $(100, 0, 100)$  cm and (b)  $(10, 0, 10)$  cm from the spacecraft mass center. Curves (1) and (2) in each graph refer to different atmospheric drags assumed for each trajectory. (1) - corresponds to  $0.2 \mu\text{g}$  and (2) to  $0.02 \mu\text{g}$ . The vertical dashed lines show the relative size of the PAS tube diameter. The circle is a cross section of the 4mm sphere drawn to the same scale as the graph axes.

### STS 50 (USML-1) data

The following acceleration measurements were made on STS-50 (USML-1) with PAS (Flight Deck) days 1-5 and OARE (Orbital Acceleration Research Experiment) on MET days 2&3, and a single data point from PAS taken near the Crystal Growth Furnace (CGF) on day 6. The PAS data represents an average over 8 measurements. Both the Flight Deck and OARE data are extrapolated to the CGF location. Both OARE and PAS data indicate that besides the gravity gradient and atmospheric drag effects, for the USML-1 mission there was an additional contribution to the quasi-steady residual acceleration vector. It contributed, approximately, an additional  $0.5 \mu\text{g}$  acceleration along the negative x-direction (body coordinates see Fig. 6). This cannot be entirely accounted for by the Flash Evaporation System (FES)<sup>1</sup>. Note that the frame of reference of the residual accelerations presented here is taken to be the spacecraft frame and that the coordinate system refers to the "Orbiter body coordinates" (see Fig. 6).

All acceleration vectors are represented in the form  $\mathbf{a} = (a_x, a_y, a_z)$ , where the components of  $\mathbf{a}$  represent the projections of the total acceleration vector onto the x-,y- and z-body axes.

### Flight deck accelerations STS-50

Table 2. STS-50 Flight deck data, days 1-5

U [cm s <sup>-1</sup> ]	acceleration [cm s <sup>-2</sup> ]	acceleration [g]
$2.43 \times 10^{-2}$	$4.34 \times 10^{-3}$	$4.43 \times 10^{-6}$
$2.52 \times 10^{-2}$	$4.48 \times 10^{-3}$	$4.57 \times 10^{-6}$
$2.73 \times 10^{-2}$	$4.87 \times 10^{-3}$	$4.97 \times 10^{-6}$
$2.49 \times 10^{-2}$	$4.44 \times 10^{-3}$	$4.53 \times 10^{-6}$
$2.38 \times 10^{-2}$	$4.23 \times 10^{-3}$	$4.32 \times 10^{-6}$
$2.57 \times 10^{-2}$	$4.58 \times 10^{-3}$	$4.67 \times 10^{-6}$
$2.54 \times 10^{-2}$	$4.53 \times 10^{-3}$	$4.62 \times 10^{-6}$
$2.56 \times 10^{-2}$	$4.58 \times 10^{-3}$	$4.67 \times 10^{-6}$

Maximum deviation in values 12% (occurred on same day)

Readings were taken in Flight deck from days 1-5, and on remaining days measurements were made in the spacelab. As can be seen from the table below, these readings produced consistent data and the PAS appeared to work best here. The flight deck readings form the best data set. Only the readings taken near the CGF in spacelab produced a usable measurement. The

<sup>1</sup>R. Blanchard, OARE STS-50 Flight Data, final report, December, 1992.

remaining readings in spacelab were either disturbed too frequently to yield useful data or the excursion of the sphere was too small. Table 2 gives the sphere's velocities and associated acceleration for the flight deck.

At the flight deck location, the direction of the acceleration was chiefly along the positive x-body axis of the orbiter. This is consistent at this location with the expected domination of the gravity gradient acceleration. Since we know the variation of the gravity gradient acceleration as a function of location the flight deck results can be extrapolated to the CGF location.

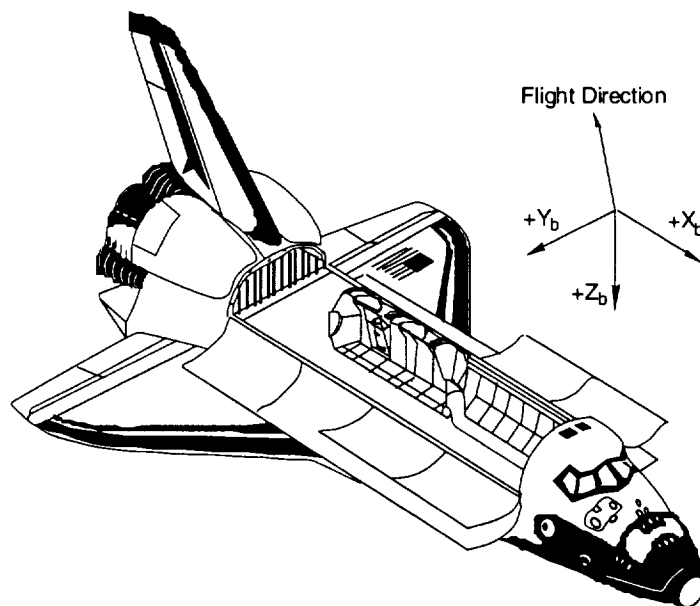


Fig. 6 Orbiter coordinate system.

*Accelerations at the CGF location (extrapolated)*

The acceleration,  $\mathbf{a}^*$ , calculated from extrapolated PAS Flight Deck data (MET days 2&3) is

$$\mathbf{a}^* = (-0.57, 0.14, -0.46) \mu g$$

The vector was calculated by calculating subtracting the gravity gradient acceleration for the PAS flight deck location from the measured acceleration and adding back the gravity gradient for the CGF location. This vector is illustrated in Fig.7, and shows that the vector is tilted away from the CGF axis by about  $15^\circ$  in the y-z plane. The tilt direction is toward positive y. In the x-z plane the vector is tilted away from the CGF axis by about  $50^\circ$  toward negative x. The PAS measurement is compared to the two sets of OARE data given below. Each set has a mean vector and a maximum and minimum magnitude vector.

Table 3. OARE data

set#1, FES off	Mean [ $\mu\text{g}$ ]	Max [ $\mu\text{g}$ ]	Min [ $\mu\text{g}$ ]
$\mathbf{a}_x$	-0.23	0.1	-0.5
$\mathbf{a}_y$	0.12	0.4	-0.1
$\mathbf{a}_z$	-0.75	-0.3	-1.0

set#2 , FES on	Mean [ $\mu\text{g}$ ]	Max [ $\mu\text{g}$ ]	Min [ $\mu\text{g}$ ]
$\mathbf{a}_x$	-0.6	-0.2	-0.8
$\mathbf{a}_y$	0.12	0.4	-0.1
$\mathbf{a}_z$	-0.4	-0.1	-0.65

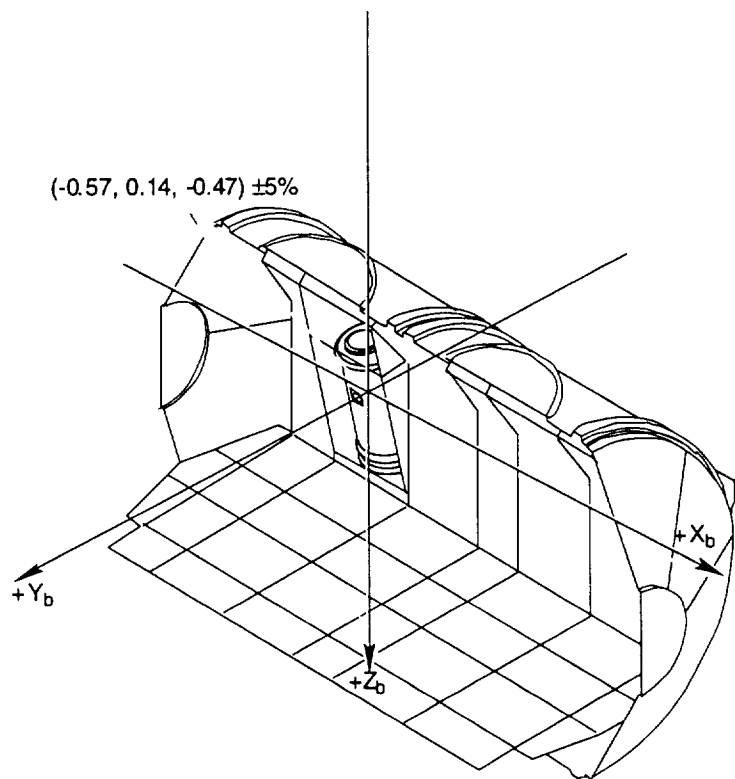


Fig. 7 PAS flight-deck measurements extrapolated to CGF location

The reading taken with PAS near the CGF yielded a magnitude of approximately  $0.6 \mu\text{g}$ . The orientation of the tube was directed primarily along the negative x-axis, and tilted in toward the CM about 15 degrees (this is compatible with the (x,y) components of the acceleration measured in the Flight Deck and indicates that the gravity gradient component in the negative x-direction was augmented by an additional acceleration of about  $0.5 \mu\text{g}$  magnitude, and that the drag was much

smaller than  $0.5 \mu\text{g}$ . The question is how much smaller? Here the PAS measurement made near CGF is inconclusive. The ball excursion distances were small, 1 cm, compared to 7 cm in the Flight Deck. The reason for this was that the intermittent vernier firings disturbed the ball motion at 3-5 minute intervals. Only one reliable reading was obtained near the CGF and while the magnitude is a reliable measure, the orientation results are questionable when one considers the ball radius is such that excursions of 3-6 cm are necessary to distinguish the orientation of the residual acceleration vector. (A back-up accelerometer tube with a larger radius ball that would have moved further between vernier firings was available. Unfortunately, circumstances did not permit transmittal of a request for the tubes to be swapped).

In summary, from the STS-50 we found that

- The PAS data and the OARE data both indicate that the net acceleration vector was not generally aligned with the CGF axis. If the drag had been  $1 \mu\text{g}$  or greater then the residual vector would have been closer to the CGF axis, although atmospheric density fluctuations will cause continuous orientation changes.

- Since the PAS location was displaced from the CGF along the x-axis the resultant vector would be expected to be oriented differently from the acceleration vector at the CGF due to gravity gradient effects.

- The resultant vector at CGF would only have lined up with the CGF axis if the drag had been  $10^{-6} \text{ g}$ . Had this been the case PAS would also have shown this orientation since drag would have dominated the gravity gradient. However, two things are apparent from CGF and OARE measurements:

- The gravity gradient acceleration along the x-axis is augmented by a  $0.5 \mu\text{g}$  acceleration acting along negative x. This has the effect of tilting PAS away from the CGF axis.

- According to OARE and the PAS Flight Deck measurements, the actual drag was about  $0.5 \mu\text{g}$  and OARE shows that at times it was lower. Under these conditions (even without the extra x-acceleration) the resultant acceleration vector would not have been aligned with the furnace axis but would be tilted at 25 degrees from the CGF toward positive y.

## Conclusions

The passive accelerometer system (PAS), although simple in its design and operation has been shown to yield useful information about the acceleration environment on board the MIR space station and on the orbiter Columbia on STS-50 (USML-1). Both the MIR and STS-50 data sets, PAS yielded intriguing results. Measurements on MIR suggest that there are periods of time in excess of 15 minutes for which the quasi-steady acceleration may *locally* be below  $1 \mu\text{g}$ . Two possible explanations for this have been put forward. One is that the measurement locations were

within 1 meter of the effective mass center of the MIR. This explanation awaits confirmation of the approximate location of the MIR mass center during this time period. Further analysis will be done upon receipt of the PAS video sequences. A journal publication is in preparation and will be completed when the data concerning the MIR mass center is obtained and when the video has been analyzed.

#### Acknowledgments

Astronaut John Blaha's efforts and patience in obtaining the PAS data are gratefully acknowledged. The enthusiastic participation of the USML-1 crew and NASA's Glovebox support team during the STS-50 mission is also acknowledged..

#### References

- [1] L. D. Landau and E. M. Lifshitz, Fluid Mechanics, Course of Theoretical Physics, Volume 6 (Pergamon, Oxford, 1979) p. 63.
- [2] J.I.D. Alexander, and C. A. Lundquist, AIAA Journal 26 (1988) 34.
- [3] J.I.D. Alexander, and C. A. Lundquist, J. Astr. Sci. 35 (1987) 193.
- [4] A. W. Francis, Physics 4 (1933) 403.